CONF-950804--2

FRACTURE BEHAVIOR OF SHALLOW CRACKS IN FULL-THICKNESS CLAD BEAMS FROM AN RPV WALL SECTION*

J. A. Keeney, B. R. Bass, and W. J. McAfee

Oak Ridge National Laboratory, Oak Ridge, Tennessee, USA

TJ

DISCLAIMER

ABSTRACT

A testing program is described that utilizes full-thickness clad beam specimens to quantify fracture toughness for shallow cracks in weld material for which metallurgical conditions are prototypic of those found in reactor pressure vessels (RPVs). The beam specimens are fabricated from an RPV shell segment that includes weld, plate and clad material. Metallurgical factors potentially influencing fracture toughness for shallow cracks in the beam specimens include material gradients and material inhomogeneities in welded regions. The shallow-crack clad beam specimens showed a significant loss of constraint similar to that of other shallow-crack single-edge notch bend (SENB) specimens. The stress-based Dodds-Anderson scaling model appears to be effective in adjusting the test data to account for in-plane loss of constraint for uniaxially tested beams, but cannot predict the observed effects of out-of-plane biaxial loading on shallow-crack fracture toughness. A strain-based dual-parameter fracture toughness correlation (based on plastic zone width) performed acceptably when applied to the uniaxial and biaxial shallow-crack fracture toughness data.

1 INTRODUCTION

Evaluations of RPV integrity under pressurized-thermal-shock (PTS) loading are based on the Marshall flaw distribution [1], U.S. Nuclear Regulatory Commission (NRC) Guide 1.154 [2], and data from deep-crack fracture toughness specimens. The Marshall flaw distribution predicts more small than large flaws, while NRC Regulatory Guide 1.154 requires that all flaws be considered as surface flaws. Probabilistic fracture-mechanics (PFM) analyses of RPVs indicate that a high percentage of the cracks that initiate in cleavage, initiate from shallow flaws [3]. Because the postulated existence of shallow flaws has a dominant influence on the results of PFM analyses, the shallow surface crack is of major importance in RPV structural integrity assessments.

This paper describes preliminary results from a Heavy-Section Steel Technology (HSST) testing program designed to quantify fracture toughness for shallow cracks in weld material for which metallurgical conditions are prototypic of those found in RPVs. In the initial phase of the investigation, three full-thickness clad beam specimens taken from the RPV of a canceled nuclear plant were tested to determine the influence of metallurgical gradients, weld inhomogeneities and the cladding process on the fracture toughness of material containing shallow cracks. Through-clad shallow cracks in these beams were located in the weld material joining together two plate material shell segments. Comparison of results from these tests with those from homogeneous

*Research sponsored by the Office of Nuclear Regulatory Research, U.S. Nuclear Regulatory Commission under Interagency Agreement 1886-8011-9B with the U.S. Department of Energy under Contract DE-AC05-84OR21400 with Martin Marietta Energy Systems, Inc.

shallow-crack test specimens [4] provide an opportunity to quantify effects of some near surface conditions on fracture toughness.

The following sections provide a summary of the HSST full-thickness clad beam testing program and analyses of the test data. Applications of the stress-based constraint characterizations developed by O'Dowd and Shih [5] and by Dodds and Anderson [6] to the clad beam data are also included. Finally, a summary with preliminary conclusions and a review of future plans are given.

2 FULL-THICKNESS CLAD BEAM TESTING PROGRAM

2.1 Details of Test Specimen

The full-thickness clad beam specimens were fabricated from an RPV shell segment that was available from a canceled pressurized-water reactor plant. The RPV material is A 533 B steel with a stainless steel clad overlay on the inner surface. The shell segment contains three submerged-arc welds (two circumferential and one longitudinal). A through-clad crack was machined in the beam (shown in Fig. 1) using the wire electro-discharge machining process. The final dimensions and material properties are listed in Tables 1 and 2.

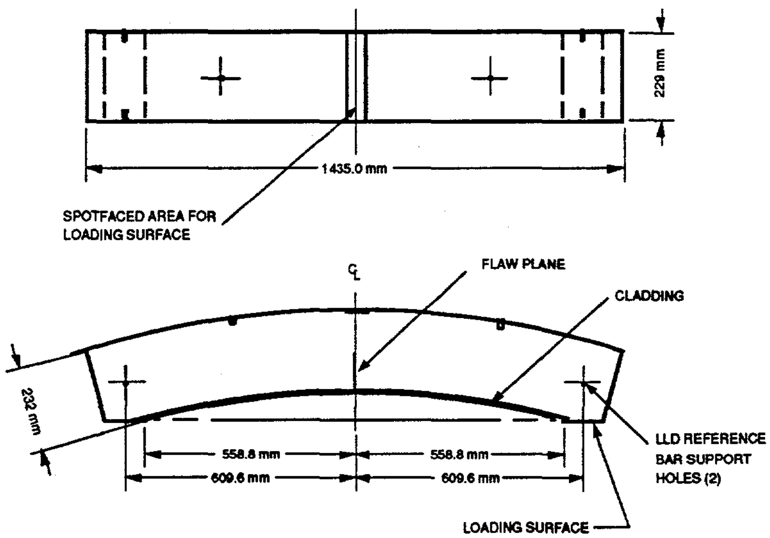

Fig. 1. Sketch of full-thickness clad beam specimen.

Table 1. Parameters defining specimen geometry of full-thickness clad beam specimens

	CB-1.1[a]	CB-1.2	CB-1.3
Load span, S (mm)	1219.2	1219.2	1219.2
Thickness, B (mm)	230.2	230.2	229.6
Width, W (mm)	225.7	224.3	224.3
Crack depth[b], a (mm)	117.5	10.8	23.7
Ratio, a/W	0.50	0.05	0.10

[a]Used as development beam.

[b]Final depth after fatigue precracking.

Table 2. Material properties at test temperature of –25°C

	Base metal	Weld metal	Clad metal
Modulus of elasticity (E), MPa	200,000	200,000	152,000
Poisson's ratio (ν)	0.3	0.3	0.3
Yield stress (σ_0), MPa	440	599	367
Ultimate stress (σ_u), MPa	660	704	659
NDT, °C		–50	

2.2 Test Procedures and Results

The full-thickness clad beam specimens were instrumented with crack-mouth-opening (CMOD) and load-line (LLD) displacement gages and tested in three-point bending [9]. Each specimen was cooled to the test temperature (–25°C) and then loaded to fracture under stroke control. The load (P) vs displacement curves for each of the three beams are shown in Figs. 2(a) and (b) for LLD and CMOD, which depict the inelastic behavior in the shallow-crack specimens. The conditions of each specimen at failure are listed in Table 3. The plastic component of the area under each P vs displacement curve (defined as U_{pl} for LLD and A_{pl} for CMOD) and the corresponding η-factors, η_{pl}^{ℓ} and η_{pl}^{c}, are also included in Table 3.

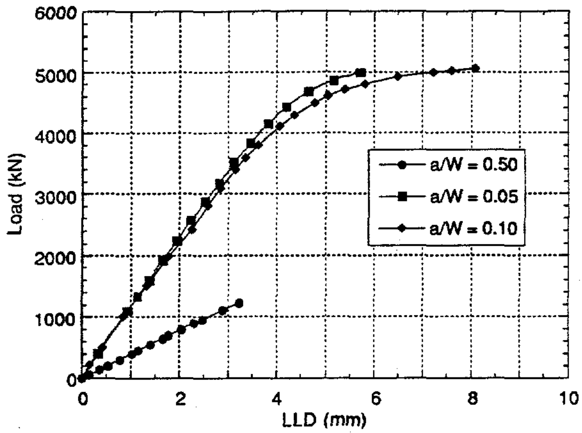

(a)

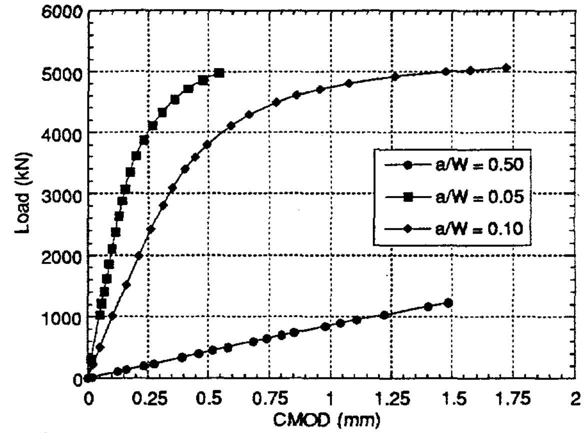

(b)

Fig. 2. Load vs displacement response for clad beam specimens: (a) LLD and (b) CMOD.

Table 3. Summary of results at failure from the full-thickness clad beam testing program

	CB-1.1	CB-1.2	CB-1.3
a/W	0.50	0.05	0.10
P, kN	1232.5	5002.3	5060
LLD, mm	3.236	5.767	8.083
CMOD, mm	1.485	0.567	1.718
U_{pl}, kN-mm	135	6427	16879
A_{pl}, kN-mm	88	1473	5486
η_{pl}^{ℓ} (η_{pl}^{c})	1.37 (2.26)	0.79 (4.16)	1.05 (4.08)
Fracture toughness			
J_{el}, kN/m	131.3	110.6	230.5
K_I, MPa$\sqrt{m}$	173.0	154.5	223.1
P vs CMOD			
J_{pl}, kN/m	8.1	124.7	486.0
Total J, kN/m	139.4	235.3	716.5
K_{Jc}, MPa$\sqrt{m}$	173.5	225.4	393.3
P vs LLD			
J_{pl}, kN/m	7.4	103.8	384.8
Total J, kN/m	138.7	214.4	615.3
K_{Jc}, MPa$\sqrt{m}$	173.1	215.2	364.5

3 CLAD BEAM POSTTEST ANALYSES

3.1 Finite-Element Analysis

Two-dimensional plane-strain elastic-plastic analyses were performed on the clad beam specimens using ABAQUS [10]. A one-half section of the complete clad beam specimen illustrated in Fig. 1 is represented in the model of Fig. 3 (a/W = 0.5). The model has a highly refined mesh in the crack-tip region [Fig. 3(c)] to provide resolution of stress fields in front of the crack. The model consists of 3712 nodes and 1155 eight-node isoparametric elements. Material properties used for the analyses were taken from Table 2 and from the true stress vs true plastic-strain curves (Fig. 4).

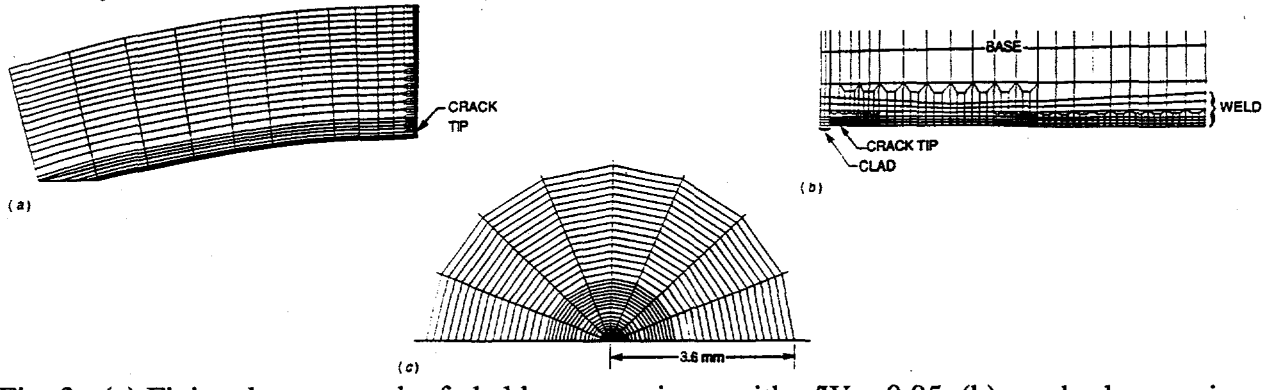

Fig. 3. (a) Finite-element mesh of clad beam specimen with a/W = 0.05, (b) crack-plane region, and (c) crack-tip region.

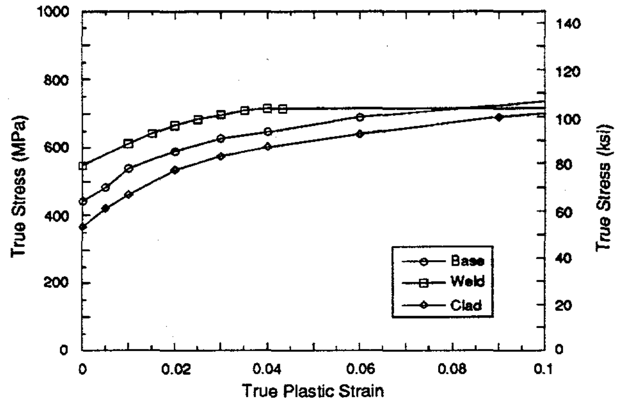

Fig. 4. Material representation for clad beam at T = –25°C.

3.2 Toughness Estimation Techniques

The two techniques [4, 7-8] used to determine the critical J are based on the "work" at the crack tip as measured by the area under the P–displacement curves. The methods require an η-factor, which relates work at the crack tip to the plastic portion of the crack-driving force. The first method of estimating J uses the P vs LLD test record. The J-integral is divided into elastic and plastic terms:

$$J = J_{el} + J_{pl} \text{ , where} \quad (1)$$

$$J_{pl} = \left(\eta_{pl}^{\ell} U_{pl}\right) / Bb, \quad (2)$$

and U_{pl} is the plastic component of the area under the P vs LLD curve, B is specimen thickness, b is the remaining ligament (W-a). Finite-element analysis provides values of η_{pl}^{ℓ} as a function of U_{pl} for each loading and specimen configuration. The U_{pl} value from the measured P vs LLD curve and the corresponding value of η_{pl}^{ℓ} for each test at cleavage initiation are included in Table 3. The second technique for determining the critical J-integral [11] uses the plastic component of the area under the P vs CMOD curve (A_{pl}) to calculate J_{pl} (values of A_{pl} and η_{pl}^{c} are listed in Table 3).

3.3 Constraint Analyses

One of the methods used to assess the effects of shallow-crack depths on crack-tip stress triaxiality is the J-Q methodology [4, 7-8], in which Q measures the departure of the opening-mode stress (σ_{yy}) from the reference plane-strain small-scale yielding (SSY) solution, normalized by σ_0 [5].

Results for the deep-crack specimen (CB-1.1) are employed as an approximation to the SSY reference solution. Analyses [4] have shown that $Q \approx 0$ for the deep-crack specimens under these loading conditions, and is supported by results shown in Fig. 5(a) for CB-1.1. The opening-mode stresses ahead of the crack tip for the shallow-crack clad beam specimens [Fig. 5(b)] exhibit an essentially uniform deviation from the SSY solution. Both specimens were found to have Q values [at $r/(J/\sigma_0) = 2$] of about -0.78 at failure, which represents a significant loss of constraint. This Q value is similar to values for the shallow-crack SENB specimens [4] ($Q \approx -0.70$).

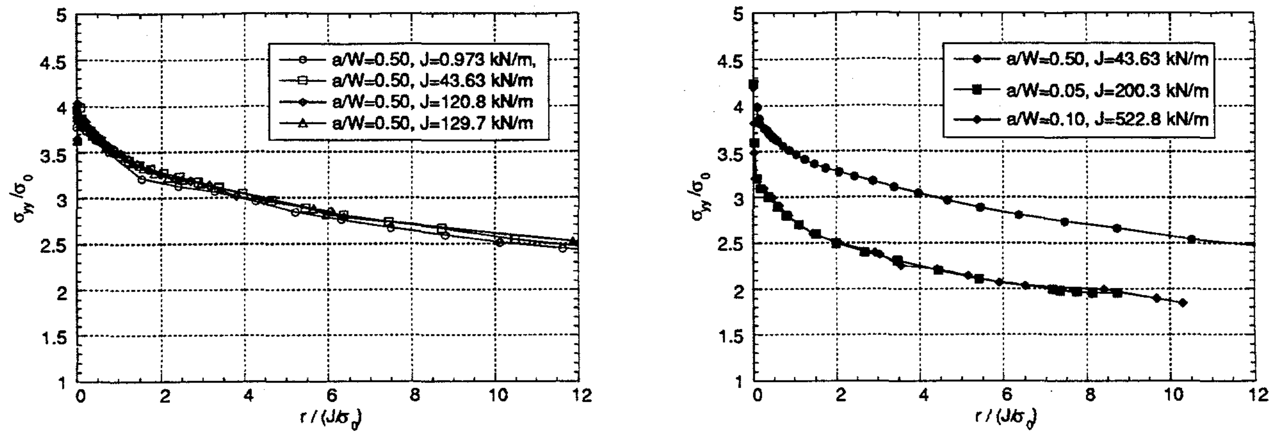

(a) (b)

Fig. 5 Distributions of normalized opening-mode stress for clad beam specimens as a function of applied J: (a) a/W = 0.50, (b) at a/W of 0.50, 0.05, and 0.10.

3.4 Fracture Toughness Scaling Model

The stress-based Dodds-Anderson (D-A) scaling model [6] analyzes constraint conditions by utilizing the area within principal stress contours to correlate toughness values from finite-body geometries with SSY conditions. The D-A scaling model was used to investigate in-plane constraint loss in the clad beam specimens. Fracture toughness data from the clad beam and shallow-crack [8] programs are shown in Fig. 6(a) as a function of (T – NDT), which indicates an increase in mean toughness and data scatter for shallow cracks due to decreased constraint.

Using the D-A [6] results, Wallin [12] has quantified in-plane constraint loss by the equation:

$$J_0 \approx J_{FB} / \{1 + [A \cdot J_{FB}/(a \cdot \sigma_0)]^B\} , \tag{3}$$

where J_0 is the SSY or reference value of J, J_{FB} is the value of J in the finite-body geometry, and A and B are constants based on the hardening exponent. The SSY value (J_0) was computed from Eq. (3) using N = 10. The K_0 results for the clad beam and SENB [8] programs are shown in Fig. 6(b), and indicate no toughness increase associated with the shallow-crack specimens. The model appears to be effective in adjusting the test data to account for in-plane loss of constraint.

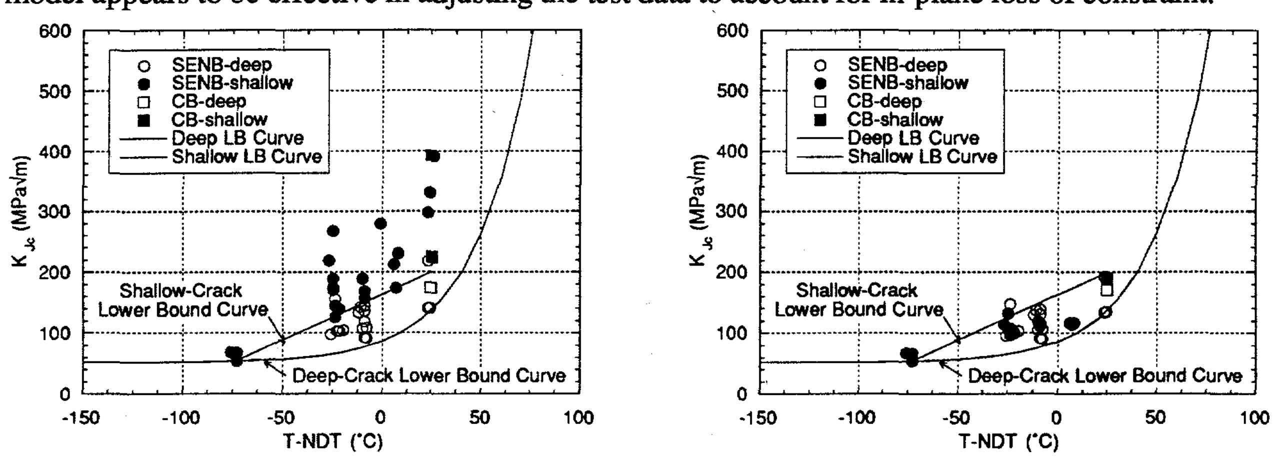

(a) (b)

Fig. 6 Fracture toughness vs T – NDT: (a) fracture toughness, (b) SSY toughness (K_0).

4 CONCLUSIONS

While stress-based dual parameter fracture toughness correlations have been successful for uniaxially tested beams, applications [8] demonstrate that they cannot predict the observed effects of out-of-plane biaxial loading on shallow-crack fracture toughness. The stress-based correlations utilize the in-plane stresses at the crack tip which are not influenced by out-of-plane biaxial loading. A strain-based dual-parameter fracture toughness correlation (based on plastic zone width) [13] performed acceptably when applied to uniaxial and biaxial shallow-crack fracture toughness data.

Recently two additional clad beam tests were tested with the objective of duplicating the shallow-crack tests in weld metal. Shallow-crack fracture toughness results from these specimens should provide additional data for a better understanding of the effects of metallurgical conditions in the region of the clad HAZ. Additional specimens will be available for testing of shallow cracks in the A 533 B plate material and to respond to further testing needs derived from results of the existing test matrix.

REFERENCES

[1] W. Marshall et al., "An Assessment of the Integrity of PWR Pressure Vessels," UKAEA Study Group Reports, March 1982.

[2] U. S. Nuclear Regulatory Commission Regulatory Guide 1.154, "Format and Content of Plant-Specific Pressurized Thermal Shock Safety Analysis Reports for Pressurized Water Reactors", January 1987.

[3] R. D. Cheverton and D. G. Ball, Martin Marietta Energy Systems, Inc., Oak Ridge Natl. Lab., "Pressurized-Thermal-Shock Evaluation of the Calvert Cliffs Nuclear Power Plant," pp. 201-244, NUREG/CR-4022, (ORNL/TM-9408), September 1985.

[4] T. J. Theiss, D. K. M. Shum, and S. T. Rolfe, Martin Marietta Energy Systems, Inc., Oak Ridge Natl. Lab., "Experimental and Analytical Investigation of the Shallow-Flaw Effect in Reactor Pressure Vessels," NUREG/CR-5886, (ORNL/TM-12115), July 1992.

[5] N. P. O'Dowd and C. F. Shih, Naval Surface Warfare Center, "Two Parameter Fracture Mechanics: Theory and Applications," USNRC Report NUREG/CR-5958 (CDNSWC/SME-CR-16-92), February 1993.

[6] T. L. Anderson and R. H. Dodds, "Specimen Size Requirements for Fracture Toughness Testing in the Ductile-Brittle Transition Region," *J. Test. Eval.* 19, 123-134 (1991).

[7] T. J. Theiss et al., Martin Marietta Energy Systems, Inc., Oak Ridge Natl. Lab., "Initial Results of the Influence of Biaxial Loading on Fracture Toughness," NUREG/CR-6036, (ORNL/TM-12349), June 1993.

[8] B. R. Bass, J. W. Bryson, T. J. Theiss, and M. C. Rao, Martin Marietta Energy Systems, Inc., Oak Ridge Natl. Lab., "Biaxial Loading and Shallow-Flaw Effects on Crack-Tip Constraint and Fracture Toughness," NUREG/CR-6132, (ORNL/TM-12498), January 1994.

[9] J. A. Keeney, B. R. Bass, W. J. McAfee, and S. K. Iskander, Martin Marietta Energy Systems, Inc., Oak Ridge Natl. Lab., "Preliminary Assessment of the Fracture Behavior of Weld Material in Full-Thickness Clad Beams," NUREG/CR-6228, (ORNL/TM-12735), October 1994.

[10] *ABAQUS Theory Manual*, Version 5–3, Hibbit, Karlson, and Sorensen, Inc., Providence, RI, 1993.

[11] M. T. Kirk and R. H. Dodds, Jr., Department of Civil Engineering, University of Illinois, "J and CTOD Estimation Equations for Shallow Cracks in Single Edge Notch Bend Specimens," USNRC Report NUREG/CR-5969 (CDNSWC/SME-CR-17-92), July 1993.

[12] K. Wallin, "Statistical Aspects of Constraint with Emphasis on Testing and Analysis of Laboratory Specimens in the Transition Region," *Constraint Effect in Fracture, ASTM STP 1171*, E. M. Hackett, K. H. Schwalbe, and R. H. Dodds, Eds., ASTM, Philadelphia, 1993.

[13] W. E. Pennell, B. R. Bass, J. W. Bryson, and W. J. McAfee, "An Interim Report on Shallow-Flaw Fracture Technology Development," Fatigue, Flaw Evaluation and Leak-Before-Break Assessments, Pressure Vessel & Piping Conference, Honolulu, Hawaii, July 1995.